

On the Strength of Oceanic Fracture Zones and Their Influence on the Intraplate Stress Field

ERIC A. BERGMAN¹ AND SEAN C. SOLOMON²

Department of Earth, Atmospheric, and Planetary Sciences, Massachusetts Institute of Technology, Cambridge

We use the locations and source mechanisms of oceanic intraplate earthquakes to test the hypothesis that the strength of oceanic fracture zones is less than that of normal oceanic lithosphere. If fracture zones are weaker than the surrounding lithosphere, they should be sites of concentrated intraplate seismicity, and the lithospheric stress field should be perturbed in their vicinity. The 77 earthquakes selected for the study have well-determined focal mechanisms and epicenters in regions where fracture zones are well mapped. We have searched for dependence of faulting style, fault orientation, or principal stress direction on the distance from the nearest fracture zone. If fracture zones were generally weaker than the surrounding lithosphere, one of the principal horizontal stresses would be oriented nearly perpendicular to the fracture zone; we find no evidence that principal stresses near fracture zones are oriented preferentially in this manner. There is a slight tendency for earthquakes to occur near fracture zones, and patterns of fault orientation and sense of slip support the view that differential cooling and horizontal contraction on fracture zones may contribute seismogenic stress. These patterns are not demonstrable at high significance, however. If oceanic transform fault zones are weak relative to the surrounding lithosphere, these results suggest that the strength of the fracture zones increases within a few million years after cessation of transform motion to levels comparable with that of normal oceanic lithosphere.

INTRODUCTION

In the long-running debate over the level of shear stress in the lithosphere a new round of discussion has been stimulated by the observation that the maximum principal horizontal stress is nearly orthogonal to the San Andreas fault in central California, resulting in a low level of resolved shear stress on the fault [Mount and Suppe, 1987; Zoback *et al.*, 1987]. This orientation represents a 30°–40° clockwise rotation from that of the regional stress field at distances greater than 100–200 km from the fault. To explain this observation, it has been proposed that the lithosphere is much weaker in the fault zone than in the interior of the plate. An attractive feature of this hypothesis is that it reconciles indications of kilobar-level stresses in the interiors of plates [Hanks and Raleigh, 1980] with heat flow observations which place a much lower (~100 bars) upper bound on shear stress along the San Andreas fault [Brune *et al.*, 1969; Lachenbruch and Sass, 1980]. In opposition to the hypothesis, Scholz [1989] has criticized both the data chosen to infer the state of stress near the San Andreas fault and the lack of a plausible mechanism to weaken the fault zone. Hickman [1991] provides a thorough review of these debates.

A corollary of the hypothesis that the San Andreas fault zone is substantially weaker than the interior of the North American plate is that all transform plate boundaries are similarly weakened with respect to the surrounding lithosphere. Several lines of evidence point, by analogy, to a low level of shear stress at oceanic transforms. Lachenbruch and Thompson [1972] and Froidevaux [1973] found that the

orthogonality of the ridge-transform system could be explained through a minimum energy principle if the resistive forces at transforms are less than those at spreading ridges. Wax model experiments contradicted these results, however, and led Oldenburg and Brune [1975] to the conclusion that the resistive forces at the ridge axis were much smaller than those at the transform; the distribution of seismic energy release on ridges and transforms favors this latter view. In these model experiments, ridges and transforms are orthogonal only if the level of friction on the transform is less than the shear strength of the surrounding material.

Focal mechanisms of microearthquakes near the Kane transform fault, at 24°N on the Mid-Atlantic Ridge, indicate that the minimum horizontal principal stress axis outside the principal transform displacement zone is oriented nearly perpendicular to the transform [Wilcock *et al.*, 1990]. The reduced level of shear stress on the transform implied by this observation could be caused by a reduction in the intrinsic strength of the material in the fault zone. Turcotte [1974] and Collette [1974] suggested that transform faults form largely to relieve ridge-parallel extensional stresses caused by thermal contraction; this view is supported by Sandwell [1986] on the basis of the observed linear correlation between transform spacing and spreading rate. Extensional strain across transforms could facilitate water circulation in the fault zone, causing a reduction in strength through chemical alteration and increased pore pressure. In this way, several mechanisms could be acting to lower the shear strength of oceanic transforms.

The San Andreas example shows that material in a transform fault zone may be substantially weakened relative to the surrounding lithosphere even where the stress field is characterized by fault-normal compression. A similar situation has been reported for an oceanic transform. From comparisons of a model of the stress field of the Gorda plate with earthquake locations and focal mechanisms, Denlinger [1992] found that the resistance to shear motion of the Mendocino transform must be a small fraction of the bulk

¹Now at U.S. Geological Survey, National Earthquake Information Center, Golden, Colorado.

²Now at Department of Terrestrial Magnetism, Carnegie Institution of Washington, Washington, D. C.

Copyright 1992 by the American Geophysical Union.

Paper number 92JB01076.
0148-0227/92/92JB-01076\$05.00

yield stress of the plate, even though regional stress measurements indicate a fault-normal compressional stress field along the transform.

Therefore we adopt as a working hypothesis the view that active transform plate boundaries are weak, in the sense that they support a lower level of shear stress than the surrounding lithosphere. In order for the resolved shear stress on the transform to be low, one of the principal horizontal stress axes of the regional lithospheric stress field must be at a high angle to the transform. In California this is the axis of maximum compression; at the Kane transform (and probably most oceanic transforms if thermoelastic stresses dominate) it is the axis of minimum compression. In general, the strength of a fault zone relative to the surrounding lithosphere is reflected in the degree to which it perturbs the regional stress field. The influence of a fault which penetrates the entire plate should be observable to a distance comparable to the mechanical plate thickness.

This hypothesis leads immediately to the question addressed in this study: if the shear strength of the lithosphere in an active transform domain is low, how long does it remain so after the transition to an inactive fracture zone? In a number of studies the topography and geoid signatures of nontransform limbs of oceanic fracture zones have been modeled successfully under the assumption that the elastic lithosphere is welded and is mechanically uniform across the fracture zone. For example, *Sandwell and Schubert* [1982] matched bathymetric profiles across large-offset fracture zones with a model featuring the flexural effects of differential subsidence. *Parmentier and Haxby* [1986] found that significant features of geoid anomalies across fracture zones could be matched by flexure due to thermal bending moments. However, in a more detailed study by *Wessel and Haxby* [1990] of the combined effects of thermal bending moments and differential subsidence, an improved fit to bathymetric and geoid profiles was possible if vertical slip along the fracture zone occurs for 2–4 m.y. after passing the ridge-transform intersection. The asymmetry in elevation of inside and outside corners at ridge-transform intersections also implies a rapid increase in the degree of coupling across the fault zone as it passes from the active transform to the inactive fracture zone domain [*Severinghaus and Macdonald*, 1988].

Evidence that fracture zones may remain weak for an extended period of time after passing the ridge-transform intersection is provided by observations of volcanic activity in close association with several fracture zones [e.g., *Lowrie et al.*, 1986]. Presumably such fracture zones act as preferred conduits for mantle-generated magma to ascend to shallow crustal levels. Bathymetric and gravity data on the Marquesas Fracture Zone in the south Pacific have been successfully modeled under the assumption that the plate is decoupled at the fracture zone [*McNutt et al.*, 1989]. A numerical model of the thermal contraction of young oceanic lithosphere [*Sandwell*, 1986] indicates that ridge-parallel contraction can be a significant source of stress outside the active transform region and that fracture zones will be the preferred site for accommodation of the associated strains.

Because of the close spacing of transform offsets along most portions of the mid-ocean ridge system [e.g., *Abbott*, 1986], the evolution of the strength of fracture zones has important consequences for the mechanical behavior of the lithosphere as a whole. For example, the evolution of the

ridge-transform geometry may be influenced by the strength of fracture zones in young oceanic lithosphere. As zones of weakness, fracture zones would facilitate a reorganization of the spreading geometry under the influence of changes in plate-driving forces.

Further, knowledge of the relative strength of fracture zones as a function of lithosphere age is required to guide efforts to map the global intraplate stress field. In oceanic regions, such efforts depend heavily on stress directions inferred from the focal mechanisms of intraplate earthquakes [*Sykes and Sbar*, 1973; *Richardson et al.*, 1976, 1979; *Zoback et al.*, 1989]. Several workers have noted earthquakes which may represent release of strain associated with differential contraction across fracture zones [*Anderson et al.*, 1974; *Forsyth*, 1975; *Engeln et al.*, 1986]. If such earthquakes (or any other stress measurement) are located within the region of influence of a weak fracture zone, the inferred stress axes will provide a biased sample of the regional stress field. *Sykes* [1978] suggested that intraplate seismicity may preferentially occur on zones of preexisting weakness, and *Bergman and Solomon* [1980] found that many oceanic intraplate earthquakes do occur near fracture zones. The focal mechanism of an earthquake localized on a weak, preexisting fault may be a poor indicator of the orientation of the local stress field [e.g., *McKenzie*, 1969; *Zoback et al.*, 1987].

We have investigated these issues using a carefully selected suite of oceanic intraplate earthquakes with known focal mechanisms. We seek to determine if there is any relation between the focal mechanisms and the orientation of nearby fracture zones which would suggest a significant variation in strength between fracture zones and the surrounding oceanic lithosphere.

SELECTION OF OCEANIC INTRAPLATE EARTHQUAKES

The oceanic intraplate earthquakes analyzed in this study are a subset of the catalog of contemporary in situ stress measurements compiled for the World Stress Map Project [*Zoback et al.*, 1989]. The data set is complete through 1988. The focal mechanisms are known from first-motion studies, body-waveform modeling studies, and the routine determination of centroid moment tensors (CMTs) by workers at Harvard University [e.g., *Dziewonski et al.*, 1981]. Extension of the CMT analysis to earthquakes with magnitudes as small as m_b 5.0 since 1977 [*Dziewonski et al.*, 1987] has contributed many new data for this study. Most of the events with known mechanisms occurred since the inception of the World-Wide Standardized Seismograph Network (WWSSN) in 1963, but several workers have performed source studies for larger earthquakes which occurred as early as 1925 [e.g., *Wiens and Petrov*, 1990].

Several factors would complicate the interpretation of a study based on the entire set of oceanic intraplate earthquakes with known focal mechanisms. The difficulties fall into two main categories: (1) poor resolution of the focal mechanism and (2) sampling bias from clusters of earthquakes. In the first category we include the questionable reliability of focal mechanisms determined for small, remote earthquakes from *P* wave first motions alone. This problem is particularly severe for events with dip-slip mechanisms, for which there is usually very poor control on the strike of the nodal planes. Even when waveform modeling methods

are used, the resolution of focal mechanisms for historical (pre-WWSSN) events is often compromised by the small number of stations and poorly known instrument response functions.

To eliminate earthquakes with less reliable focal mechanisms, we removed the following events from the data set: (1) earthquakes with focal mechanisms determined only from first motions, (2) earthquakes before 1962, and (3) earthquakes with seismic moment $M_0 < 7.0 \times 10^{16}$ N m. Most of the events rejected by the moment threshold criterion are CMT solutions obtained from only a small number of records with poor signal-to-noise ratios.

Sampling bias can arise when clusters of related earthquakes comprise a significant fraction of the events in the catalog. Notable examples include 36 earthquakes in the 1981–1983 Gilbert Islands swarm [Lay and Okal, 1983] for which CMT solutions are available, and 14 aftershocks of a large ($M_S = 7.4$) earthquake which occurred near the Chagos Bank in the Indian Ocean on November 30, 1983. The potential biasing effect of sites of unusually high levels of seismicity is minimized by selecting a single representative earthquake from such clusters. The catalog is thereby reduced to distinct sites of intraplate seismicity. For this purpose we regard as a single site a region whose lateral extent is comparable to the mechanical plate thickness, approximately 50 km.

We also removed from the catalog a small number of earthquakes which did not occur in normal oceanic lithosphere. These included events near continental margins, in submerged blocks of continental lithosphere, and in back-arc or marginal basins. Finally, since the study depends on our ability to estimate with confidence the distance of an earthquake from the nearest fracture zone, the data set is restricted to earthquakes where fracture zones have been adequately mapped. The issue of fracture zone mapping is discussed further below.

With the catalog culled as described above, the set of 223 oceanic intraplate earthquakes with known focal mechanisms is reduced to 77 representative earthquakes with reliable focal mechanisms in regions where major fracture zones are reasonably well mapped. These earthquakes are listed in Table 1; their epicenters are shown in Figure 1. The age of the lithosphere at the epicenter is also listed in Table 1. For an epicenter within 20 km of a fracture zone the ages on both sides are listed, with the age at the nominal epicenter given first. If the epicenter lies on the fracture zone, the younger age is given first.

RELATION TO OCEANIC FRACTURE ZONES

The basic reference used for mapping fracture zones was the General Bathymetric Chart of the Oceans series of bathymetric maps. Where fracture zone traces are inadequately delineated by the bathymetry, we determined their locations on the basis of tectonic maps by Sclater *et al.* [1980], Atwater and Severinghaus [1988a, b, c], and Cande *et al.* [1989]. These compilations rely on offsets of magnetic lineations to map fracture zone traces in many areas; Atwater and Severinghaus and Cande *et al.* also employed satellite altimetry data for this purpose. In the maps of Sclater and others, fracture zones are often extrapolated outside the regions where data were available at the time, in order to obtain complete coverage for the ocean basins. The map of

Cande *et al.* [1989] shows fracture zone traces only where they are required by the data; it was used as the first alternative to bathymetric information.

For each earthquake the distance to the nearest fracture zone and the strike of the fracture zone are listed in Table 1. We estimate an accuracy of about 3° for the strikes. Given the typical uncertainty for teleseismically determined epicenters (10–20 km) and an estimated uncertainty of 10 km for the location of the fracture zone trace, the distances in Table 1 would have standard deviations of 15–20 km. The age offset across the fracture zone is also listed where a reasonably accurate estimate could be made.

Even though the study was limited to areas where fracture zones appear to be well mapped, some of the earthquakes probably are located near unmapped fracture zones. For example, portions of the Mid-Atlantic Ridge appear to be segmented at lengths of a few tens of kilometers by small-offset or zero-offset fracture zones, but we measured distances of several hundred kilometers to the nearest major fracture zone in some cases. The strike of any such unmapped fracture zone is likely to be close to the measured strike of the fracture zone actually used to compile the data in Table 1, but the distance to the epicenter will, of course, be less. To the extent that the unmapped fracture zones have small or zero offsets and that active faults weaken as a result of mechanical action during slip, such zones are less likely to represent sites of significant weakness in the lithosphere.

ANALYSIS

For the investigation of relationships between earthquakes and fracture zones the earthquake data set is subdivided according to mechanism type. We make the common distinction between reverse, normal, and strike-slip mechanisms, but categories are also included for mixed mechanisms, those combining significant components of dip-slip and strike-slip motion. The classification is based on the slip angle λ of the focal mechanism, using the convention of Aki and Richards [1980]: reverse faulting mechanisms are defined by $\lambda = 90^\circ \pm 30^\circ$, normal faulting mechanisms are defined by $\lambda = 270^\circ \pm 30^\circ$, and strike-slip mechanisms are defined by $\lambda = 0^\circ \pm 30^\circ$ or $\lambda = 180^\circ \pm 30^\circ$. Mixed mechanisms fall between these ranges. The distribution by mechanism type is shown in Table 2.

The epicenters and faulting styles of intraplate earthquakes may be influenced in several ways if fracture zones are significantly weaker than the surrounding lithosphere or if they are sites of localized stress concentrations. To observe such influences, we investigate two relationships: (1) the degree to which the earthquakes tend to cluster near fracture zones and (2) the degree to which the orientations of their focal mechanisms are correlated with the strike of nearby fracture zones.

Clustering of Seismicity Near Fracture Zones

A probable consequence of the pervasive weakness of oceanic fracture zones would be a tendency for seismicity to be concentrated within these zones of weakness. Such a zone is unlikely to be wider than the seismically active zone of oceanic transforms, perhaps 10 km at most [Bergman *et al.*, 1988]. Combining the uncertainties in the locations for both fracture zones and earthquakes, an earthquake at a

TABLE 1. Representative Oceanic Intraplate Earthquakes With Known Focal Mechanisms

Date	Origin Time	Latitude, °N	Longitude, °E	Lithosphere Age	Focal Mechanism			Fracture Zone		
					Strike/Dip/Slip	Type	Reference	Distance, km	Azimuth, deg	Offset, m.y.
Aug. 6, 1962	0135	32.26	-41.03	8	288/43/315	NS	BS1	230	100	7
May 25, 1964	1944	-9.08	88.89	65	177/87/005	S	BS2	130	2	
Sept. 17, 1964	1502	44.58	-31.34	24	240/73/130	RS	WS2	850	90	10
Oct. 23, 1964	0156	19.80	-56.11	65	285/56/152	S	B1	380	90	9
Sept. 9, 1965	1002	6.51	-84.44	12/14	173/88/160	S	BS1	10	0	2
Oct. 31, 1965	1724	-14.22	95.27	66	165/68/009	S	BS2	75	358	3
Feb. 17, 1966	1147	-32.20	78.93	4/7	276/60/290	N	BNS	0	36	3
Jan. 7, 1967	0027	-48.80	112.76	3	016/41/236	NS	BS1	160	10	1
Sept. 3, 1968	1537	20.58	-62.30	>85	168/76/004	S	B1	0	115	
Sept. 14, 1968	0125	-24.45	80.41	28/35	291/48/082	R	BS2	0	30	7
Oct. 8, 1968	0743	-39.85	87.74	8	006/54/269	N	BNS	40	37	4
Aug. 8, 1969	1108	-47.76	-15.66	9	008/67/215	NS	BS1	25	80	12
Oct. 1, 1969	1710	0.78	-85.01	3/0	112/53/272	N	H1	20	3	3
Dec. 14, 1969	1837	8.20	58.49	3	317/63/061	R	H1	45	40	1
Jan. 21, 1970	1751	7.03	-104.24	3	332/41/106	R	BS1	130	85	2
March 31, 1970	1818	-3.78	69.70	8	043/83/187	S	BS1	35	40	5
April 25, 1970	0343	-6.29	69.84	11	248/85/192	S	BS1	45	48	4
Oct. 10, 1970	0853	-3.56	86.19	75/80	019/89/358	S	BS2	20	2	5
May 9, 1971	0825	-39.78	-104.87	9	025/46/104	R	BS1	330	90	2
June 26, 1971	1927	-5.18	96.90	55	014/67/019	S	BS2	125	358	12
Sept. 30, 1971	2124	-0.45	-4.89	45	079/60/074	R	B1	50	75	1
May 2, 1972	0656	5.22	-100.32	3	332/49/280	N	BS1	125	67	
Oct. 20, 1972	0433	20.60	-29.69	>90	250/79/169	S	B1	130	105	11
April 7, 1973	0300	7.00	91.32	>70	020/87/009	S	BS2	55	0	
May 3, 1973	2311	-46.14	73.22	25/30	185/50/253	N	BNS	20	44	5
June 29, 1973	0755	3.93	-85.03	10/8	353/61/169	S	BS1	10	6	2
Sept. 21, 1973	0713	-4.40	-102.10	4	015/52/272	N	B2	30	100	3
Nov. 17, 1973	1051	-1.59	69.85	9	046/51/226	NS	BS1	65	39	2
June 25, 1974	1722	-26.02	84.30	40/37	010/50/025	S	BS2	15	30	3
July 1, 1974	2311	-22.57	-10.68	15	068/29/092	R	BS1	30	78	10
Sept. 19, 1975	0337	-34.74	81.88	11	241/63/275	N	BNS	50	38	
Oct. 29, 1975	0501	4.07	-103.51	2	220/66/260	N	WS2	40	87	
March 29, 1976	0539	3.96	-85.88	10	199/82/181	S	BS1	100	6	2
Aug. 4, 1976	1400	-35.62	-14.02	17	200/63/090	R	WS2	30	80	6
Nov. 2, 1976	0713	-29.36	77.65	8	231/37/282	N	BNS	100	38	
Feb. 5, 1977	0329	-66.49	-82.45	50/55	002/42/073	R	B1	15	143	5
May 28, 1977	1510	-65.04	175.7	3/13	153/46/129	RS	CMT	0	151	10
Aug. 26, 1977	1950	-59.54	-20.59	17	091/85/175	S	BS1	60	90	9
Dec. 13, 1977	0114	17.33	-54.91	55	238/60/049	RS	B1	55	80	9
Dec. 14, 1977	0300	-33.84	57.98	27	017/50/278	N	WP1	25	3	9
March 24, 1978	0042	29.68	-67.45	125	330/44/089	R	B1	15	110	
Aug. 3, 1978	0110	-0.93	84.24	>80	261/53/090	R	BS2	160	5	
May 22, 1979	0155	-43.81	79.00	9	197/49/280	N	BNS	90	36	3
Oct. 16, 1979	2251	6.37	91.21	75	014/76/353	S	CMT	40	0	5
Dec. 13, 1979	0243	5.55	-80.48	12/10	349/75/178	S	BS1	10	6	2
Jan. 28, 1980	1446	-3.37	88.89	>60	009/68/359	S	WP2	160	4	
Nov. 1, 1980	1600	-3.18	-12.68	3	338/49/049	RS	CMT	45	78	4
Sept. 13, 1981	0919	24.84	-46.29	6	021/33/264	N	BS1	105	103	11
Sept. 24, 1981	2109	-45.76	79.83	14	142/37/247	N	BNS	80	40	2
Sept. 29, 1981	1000	-62.24	153.5	7	281/32/298	N	CMT	40	150	3
Dec. 2, 1981	1901	-15.70	88.43	>50	222/44/078	R	BS2	180	3	
Dec. 12, 1981	2331	4.95	70.21	50	060/50/307	NS	BS1	60	12	
March 22, 1982	0604	6.64	175.06	154	170/46/130	RS	CMT	90	162	7
April 10, 1982	0647	-33.98	58.11	32/23	119/34/309	NS	WP1	10	3	9
April 18, 1982	1131	-28.22	-114.06	2/3	135/45/087	R	B2	0	90	1
Oct. 15, 1982	1058	32.82	-125.94	30	282/79/017	S	CMT	100	83	3
July 31, 1983	1026	-20.12	-126.94	20	170/39/266	N	B2	60	77	7
Aug. 21, 1983	1206	3.27	87.50	75	132/23/146	RS	CMT	140	0	
Nov. 25, 1983	1956	-40.45	155.57	63	054/48/075	R	FMD	35	63	1
March 21, 1984	0827	-43.91	77.94	10/7	358/44/248	N	B2	10	36	3
Nov. 6, 1984	0758	-18.85	67.33	8	151/39/077	R	B2	65	58	3
Dec. 2, 1984	0609	20.33	-115.79	16	063/57/285	N	B2	160	83	
Oct. 6, 1985	0700	-52.02	-17.8	35	032/62/197	S	CMT	65	85	5
Dec. 14, 1985	1813	14.62	57.95	3/4	196/72/182	S	B2	0	24	1
Dec. 16, 1985	1656	-47.81	136.60	8	348/71/009	S	CMT	200	354	5
July 20, 1986	1809	-56.76	-3.56	4/12	107/59/162	S	CMT	0	90	8
March 15, 1987	1614	-10.37	91.62	52/60	224/19/105	R	CMT	0	5	8
April 5, 1987	1133	-42.36	-18.57	10	022/68/191	S	CMT	80	80	2
Dec. 22, 1987	1117	-51.54	-11.42	20/24	044/86/191	S	CMT	0	75	4

TABLE 1. (continued)

Date	Origin Time	Latitude, °N	Longitude, °E	Lithosphere Age	Focal Mechanism			Fracture Zone		
					Strike/Dip/Slip	Type	Reference	Distance, km	Azimuth, deg	Offset, m.y.
Jan. 23, 1988	2202	-15.40	-116.02	3	109/41/255	N	CMT	220	100	2
Feb. 26, 1988	0617	-37.28	48.02	9/11	318/33/089	R	CMT	10	4	2
March 5, 1988	0158	-52.24	114.60	7/9	201/69/054	RS	CMT	20	19	2
March 7, 1988	1521	41.62	152.13	125	350/54/072	R	CMT	45	155	
April 7, 1988	1814	-55.77	-15.9	53	234/71/184	S	CMT	35	115	5
July 30, 1988	1626	-33.13	83.82	22/27	246/61/302	NS	CMT	0	32	5
Aug. 21, 1988	1351	-42.83	-85.86	5/7	122/40/042	RS	CMT	10	78	2
Sept. 22, 1988	2228	23.84	-167.18	>85	053/53/134	RS	CMT	375	75	

Epicentral data are from the Bulletin of the International Seismological Centre. Origin time is given in hours and minutes. Age of the lithosphere at the epicenter is given in m.y. For events on or very close to a fracture zone the ages on both sides of the fracture zone are given (see text). Focal mechanisms are given in the order strike/dip/slip, following the convention of *Aki and Richards* [1980]. Focal mechanism types are classified as discussed in the text: *R* = reverse, *N* = normal, and *S* = strike-slip. References for focal mechanism: B1, *Bergman* [1986]; B2, E. A. *Bergman* (unpublished data, 1988); BNS, *Bergman et al.* [1984]; BS1, *Bergman and Solomon* [1984]; BS2, *Bergman and Solomon* [1985]; CMT, Harvard centroid-moment tensor solution [e.g., *Dziewonski et al.*, 1987]; FMD, *Fredrich et al.* [1988]; H1, P. Y. *Huang* (unpublished data, 1986); WS1, *Wiens and Stein* [1983]; WS2, *Wiens and Stein* [1984]; WP1, *Wiens and Petroy* [1989]; and WP2, *Wiens and Petroy* [1990]. Distance between epicenter and nearest fracture zone is in kilometers; fracture zone azimuth is given in degrees clockwise from north. Age offset of lithosphere across the fracture zone is given in m.y.

measured distance of about 30 km or less from a fracture zone could in actuality be associated with a postulated weak zone. A tendency for earthquakes to occur preferentially near fracture zones, but perhaps at greater distances, could also be caused by stresses localized on fracture zones. A total of 38% (29 of 77) of the events occurred within 30 km of a fracture zone, but the significance of this observation cannot be evaluated without considering the spacing of fracture zones in the source area of each earthquake. To do this, the distance *D* to the nearest fracture zone is normalized by *L*, the separation of the two fracture zones flanking the epicenter. If the epicenters are distributed randomly with respect to fracture zones, the distribution of the ratio *D/L* should approach a uniform distribution between values of 0 and 0.5.

Using the data in Table 2, a χ^2 test of the goodness of fit

is used to test the null hypothesis that the epicenters are uncorrelated with fracture zones. With the number of bins *N* = 5 for values of *D/L* the expected number of cases *E* in each bin is $77/N = 15.4$ if the null hypothesis is true. The statistic is calculated from

$$\chi^2 = \sum (d_i - E)^2 / E = 10.99$$

where *d_i* is the observed number of cases in each bin. The observed value is compared with tabulated values of χ^2 for 4 degrees of freedom; higher values are less consistent with the null hypothesis. A value as high as 10.99 is expected to occur with a probability α of only 0.027 if the null hypothesis is true. We therefore reject the null hypothesis at the $1 - \alpha$ (97%) confidence level and (from inspection of Table 2) conclude that the earthquakes show some tendency to occur near fracture zones.

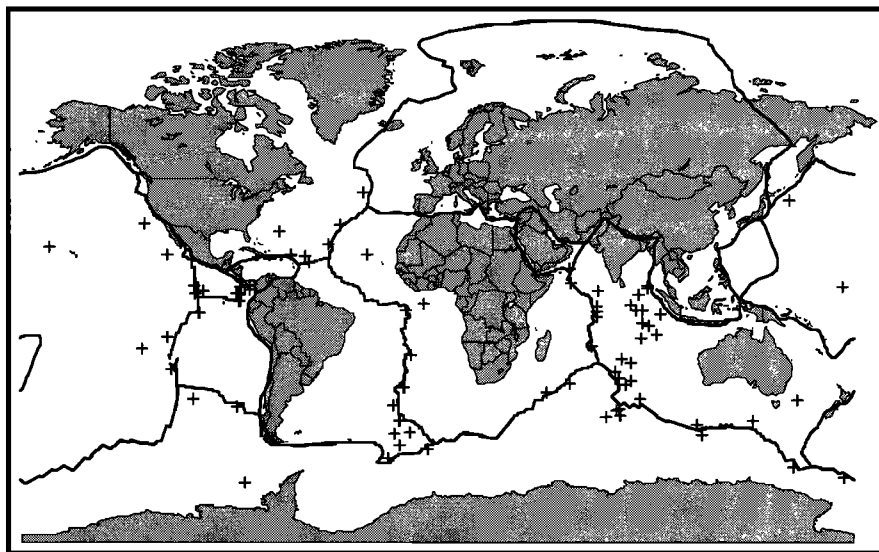


Fig. 1. Locations of oceanic intraplate earthquakes used for this study (Table 1). Events have known focal mechanisms and are located in regions where fracture zones are well mapped. Cylindrical projection. Approximate locations of major plate boundaries are also shown.

TABLE 2. Distribution of Representative Oceanic Intraplate Earthquakes by Focal Mechanism and Distance From Nearest Fracture Zone

<i>D/L</i>	Reverse	Reverse/ <i>S</i>	Strike-Slip	Normal/ <i>S</i>	Normal	Total
0.00–0.09	6	4	8	3	4	25
0.10–0.19	3	1	7	1	4	16
0.20–0.29	5	1	3	1	7	17
0.30–0.39	0	1	4	1	2	8
0.40–0.50	3	2	4	1	1	11
Total	17	9	26	7	18	77

D is the distance to the nearest fracture zone. *L* is the separation between the two fracture zones bounding the epicenter. *S* is strike-slip.

To determine if this tendency is attributable to events of a certain mechanism type, we applied the same test to several subsets of the data. *N* should be chosen so that $E > 5$ [Bulmer, 1979]; with $N = 5$, only the strike-slip category contains enough samples by itself (26) to perform a valid test. We also applied the test to the union of the reverse and mixed reverse/strike-slip categories, which contains 26 events, and the union of normal and mixed normal/strike-slip categories, which contains 25 events. Finally, we applied the test to the union of all categories with a component of dip-slip faulting (i.e., everything except pure strike-slip events). For each subset we give the observed value of χ^2 and the probability α with which a value at least this large would be expected if the null hypothesis is true (Table 3). The null hypothesis can be rejected at the 97% confidence level for the combination of dip-slip and mixed mechanisms, the same result found for the data set as a whole. The tendency for intraplate earthquakes to be clustered near fracture zones is dominated by those events with focal mechanisms characterized by a component of reverse motion. It is notable that strike-slip events show the least tendency to occur near fracture zones.

Fracture Zones and Nodal Planes

We consider next the distribution of angular differences between the strikes of fracture zones and earthquake nodal planes, performing the analysis separately for the three main mechanism types. The analysis is hindered because we do not know which nodal plane of the focal mechanism corresponds to the fault plane. To make the strongest test of the null hypothesis, that the strikes of the fault plane and fracture zone are uncorrelated, we select as the fault plane the nodal plane which is most nearly parallel to the fracture zone. This bias in data selection must be kept in mind if the test suggests that the null hypothesis should be rejected, as it does in two of the three tests.

As before, the null hypothesis is tested with the χ^2 test of the goodness of fit. The difference between the strike of the fracture zone and the presumed fault plane is converted to

the range 0° – 90° for tests of events with dip-slip mechanisms and 0° – 45° for tests of events with strike-slip mechanisms. *M* data are sorted into *N* equal-sized ($90^\circ/N$ or $45^\circ/N$) bins, with *N* chosen so that the expected number of cases in each bin $E = M/N$ is at least equal to 5. The statistic is calculated and compared with tabulated values (for *N*-1 degrees of freedom) to determine the probability α with which a value as high as the observed χ^2 would be expected if the null hypothesis is true.

Reverse faulting earthquakes. Figure 2 shows the distribution of fault plane strikes as a function of distance from the nearest fracture zone for the 26 earthquakes with reverse or mixed reverse/strike-slip mechanisms. With $N = 5$ (18° bins) the expected number $E = 5.2$. The observed value of χ^2 is 6.31, which yields $\alpha = 0.177$. The null hypothesis cannot be rejected at high confidence.

Normal faulting earthquakes. Figure 3 shows the distribution of fault plane strikes as a function of distance from the nearest fracture zone for the 25 earthquakes with normal or mixed normal/strike-slip mechanisms. With $N = 5$ (18° bins), the expected number $E = 5.0$. The observed value of χ^2 is 13.20, which yields $\alpha = 0.010$. Inspection of Figure 3 shows that the observed distribution is skewed toward small differential angles; that is, the presumed fault planes tend to be aligned with the fracture zones.

Strike-slip earthquakes. There are 42 earthquakes with focal mechanisms categorized as strike-slip or mixed, but for three of the mixed-mechanism events, neither nodal plane is within 45° of the fracture zone. These three earthquakes are not used in the following analysis. Figure 4 shows the distribution of fault plane strikes as a function of distance from the nearest fracture zone for the 39 earthquakes with strike-slip or mixed mechanisms having a nodal plane within 45° of the fracture zone. With $N = 6$ (7.5° bins), the expected number $E = 6.5$. The observed value of χ^2 is 15.32, which yields $\alpha = 0.009$. The observed distribution is skewed toward small differential angles.

The fault planes of earthquakes with a component of reverse faulting display no significant tendency to be aligned with the nearest fracture zone. Earthquakes characterized by strike-slip or normal faulting do show such a tendency at the 99% confidence level, but the significance of the χ^2 test has been overestimated because of the way the data were selected. A more conservative measure of the degree of alignment between nodal planes of normal-faulting (and mixed mechanism) events can be obtained by taking both nodal planes of each mechanism for the χ^2 test instead of the one most nearly parallel to the fracture zone. Since the nodal planes of dip-slip mechanisms tend to have similar strike

TABLE 3. Test of the Null Hypothesis That Earthquakes Are Randomly Distributed With Respect to Fracture Zones

	χ^2	α
Reverse and reverse/strike-slip	8.23	0.084
Strike-slip	3.62	0.460
Normal and normal/strike-slip	5.20	0.267
Reverse, normal and mixed	10.85	0.028

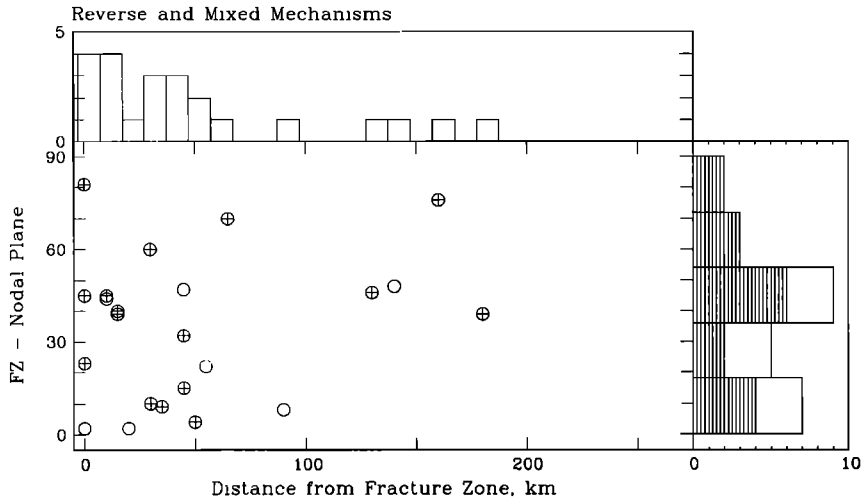


Fig. 2. Angular difference between the strike of the nearest fracture zone and the strike of the most nearly parallel nodal plane for earthquakes with reverse-faulting mechanisms (circles with crosses) or with mixed reverse/strike-slip mechanisms (open circles), as a function of the distance from the nearest fracture zone. Histograms of the distribution of events by distance from the fracture zone and by angular difference (shaded for reverse faulting events) are shown at the top and on the right-hand side, respectively.

directions, this procedure should still reveal any strong tendency for fault planes to be aligned with the fracture zones. In fact, the value of χ^2 calculated in this manner for normal or mixed normal/strike-slip mechanisms is only 3.20, for which α is 0.53. This result suggests that the correlation found above is mostly due to the events with a large component of strike-slip motion, for which one nodal plane is usually rather close to the fracture zone.

Fracture Zones and Stress Axes

We next consider the distribution of angular differences between fracture zone trends and the orientations of principal stress axes inferred from earthquake source mechanisms. Depending on whether the regional state of stress is characterized by compression or extension, either the max-

imum or minimum principal horizontal stress axis, respectively, would be expected to be oriented at a high angle to a weak fracture zone [Zoback *et al.*, 1987]. The directions of the maximum and minimum horizontal stress are taken to be the strikes of the horizontal projections of the *P* and *T* axes, respectively. While the *P* and *T* axes can be poor estimators of the principal stress axes [McKenzie, 1969], these estimates cannot be improved without additional information (e.g., identification of the fault plane). We test the null hypothesis that the orientations of principal stresses are uncorrelated with the strike of the nearest fracture zone, using the χ^2 test of the goodness of fit described previously. *P* axis. In a regional stress regime characterized by the axis of greatest principal stress being horizontal, earthquake mechanisms should have either reverse, strike-slip, or mixed

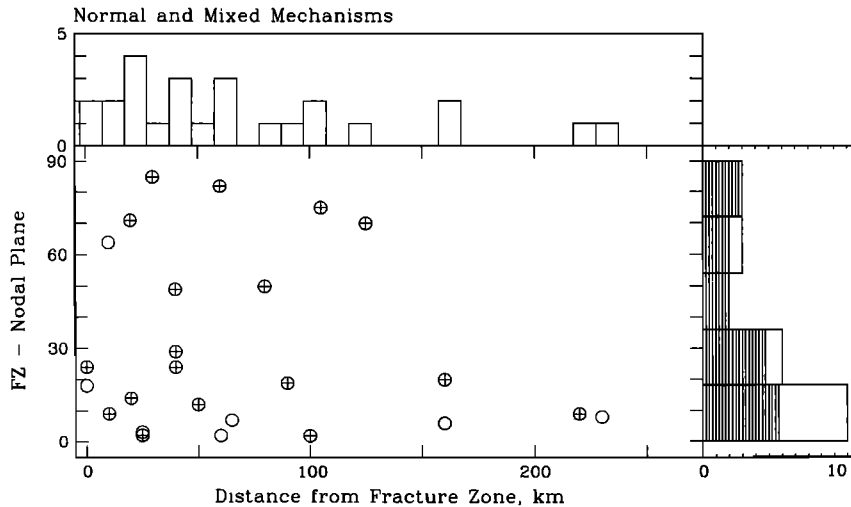


Fig. 3. Angular difference between the strike of the nearest fracture zone and the strike of the most nearly parallel nodal plane for earthquakes with normal-faulting mechanisms (circles with crosses) or with mixed normal/strike-slip mechanisms (open circles), as a function of the distance from the nearest fracture zone. Histograms of the distribution of events by distance from the fracture zone and by angular difference are shown at the top and on the right-hand side, respectively.

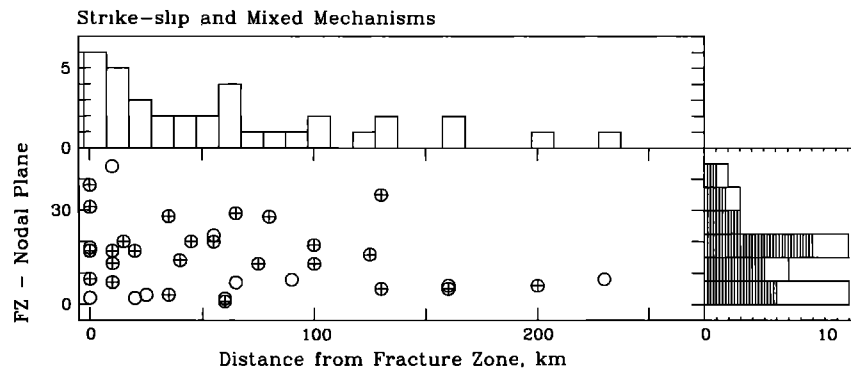


Fig. 4. Angular difference between the strike of the nearest fracture zone and the strike of the most nearly parallel nodal plane for earthquakes with strike-slip mechanisms (circles with crosses) or mixed mechanisms (open circles), as a function of the distance from the nearest fracture zone. Histograms of the distribution of events by distance from the fracture zone and by angular difference are shown at the top and on the right-hand side, respectively.

reverse/strike-slip mechanisms. The difference in strike between the maximum horizontal stress axis and the nearest fracture zone is shown for 52 events in Figure 5. With $N = 9$ (10° bins), the expected number $E = 5.78$. The observed value of χ^2 is 11.69, which yields $\alpha = 0.166$.

T axis. In a regional stress regime characterized by the axis of least principal stress being horizontal, earthquake mechanisms should have either normal, strike-slip, or mixed mechanisms. The difference in strike between the minimum horizontal stress axis and the fracture zone is shown for 51 events in Figure 6. With $N = 9$ (10° bins), the expected number $E = 5.67$. The observed value of χ^2 is 11.29, which yields $\alpha = 0.186$.

The null hypothesis (that there is no preferred orientation with respect to nearby fracture zones) cannot be rejected at a reasonable confidence level for either the maximum or minimum horizontal principal stress axes of these earthquakes.

DISCUSSION

The discussion of the results presented above is divided into three parts. The first concerns the degree to which stress directions inferred from intraplate earthquakes are correlated with the geometry of the nearby ridge-transform system. Next we consider the implications of these results for the evolution of the strength of the fracture zone lithosphere after it passes from the transform to the nontransform domain. Finally, we assess the importance of localized stresses which may accumulate near fracture zones as a result of differential cooling of the bounding lithospheric blocks.

Intraplate Stress Field

Analytical solutions to simplified models of the stresses resulting from plate cooling [e.g., *Turcotte, 1974; Sandwell, 1986*] suggest that the stress field in young oceanic litho-

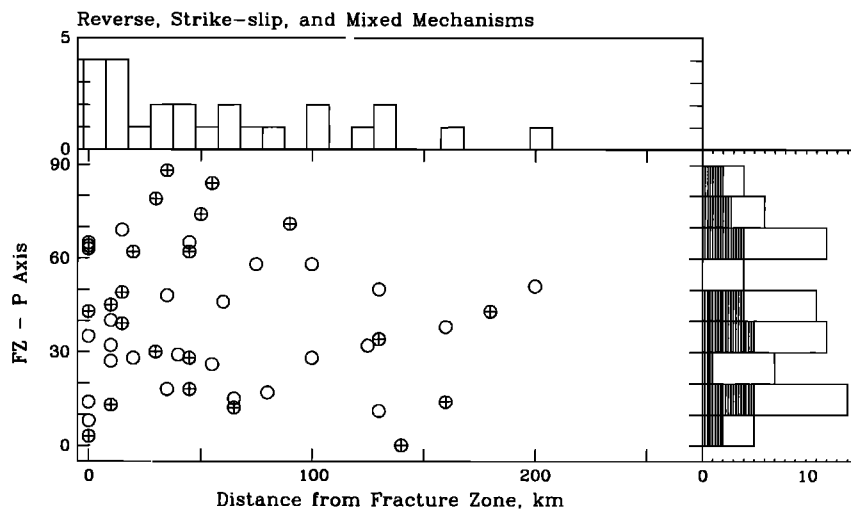


Fig. 5. Angular difference between the strike of the nearest fracture zone and the strike of the horizontal projection of the P axis for earthquakes with reverse-faulting mechanisms (circles with crosses), strike-slip mechanisms, or mixed reverse/strike-slip mechanisms (both open circles), as a function of the distance from the nearest fracture zone. Histograms of the distribution of events by distance from the fracture zone and by angular difference are shown at the top and on the right-hand side, respectively.

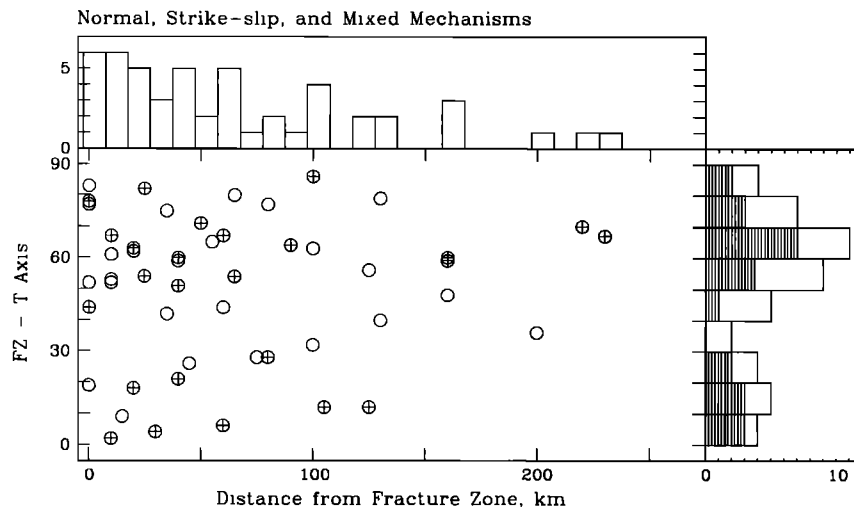


Fig. 6. Angular difference between the strike of the nearest fracture zone and the strike of the horizontal projection of the T axis for earthquakes with normal-faulting mechanisms (circles with crosses), strike-slip mechanisms, or mixed normal/strike-slip mechanisms (both open circles), as a function of the distance from the nearest fracture zone. Histograms of the distribution of events by distance from the fracture zone and by angular difference are shown at the top and on the right-hand side, respectively.

sphere should be dominated by ridge-parallel extension. Moreover, the elevation of the mid-ocean ridge system relative to the plate interior should contribute a component of compressive stress perpendicular to the ridge; the magnitude of the stress increases with lithospheric age up to an age of 80–100 m.y. [Artyushkov, 1973; Dahlen, 1981]. It is useful to ask whether the stress patterns predicted by these simple models are reflected in the earthquake data. Our catalog, like the population of oceanic intraplate earthquakes as a whole [e.g., Bergman, 1986], is heavily weighted toward young oceanic lithosphere: two thirds of the events used in this study occurred in lithosphere less than 30 m.y. old. Earthquakes with reverse mechanisms have no preferred orientation with respect to the local direction of spreading. There is only weak evidence that the nodal planes of normal-faulting events are preferentially aligned with nearby fracture zones, which would imply an alignment of the T axes as well. A direct test of the orientation of the T axes of earthquakes with appropriate mechanisms shows no correlation with ridge-transform geometry.

That observed stress orientations do not reflect the simple patterns (at wavelengths of several hundred kilometers) predicted by numerical models can be attributed to randomizing features inherent in the generation and relaxation of stresses at the shorter wavelengths appropriate to earthquakes. The accumulation of thermal stresses is strongly influenced by the detailed pattern of hydrothermal circulation, and also by any additional heat input to the young lithosphere. Stress relaxation occurs through ductile flow or faulting in the lower and upper mechanical lithosphere, respectively [Bratt *et al.*, 1985]; adjustments in the local stress field following either type of event may perturb subsequent episodes of faulting.

Strength History of Oceanic Fracture Zones

We find no evidence for systematic rotations of principal stress axes and little evidence (restricted to events with a component of reverse faulting) of enhanced seismicity on

fracture zones. This study supports other work [e.g., Severinghaus and Macdonald, 1988; Haxby and Parmentier, 1988; Wessel and Haxby, 1990] indicating that old portions of fracture zones have substantially the same strength as undisturbed lithosphere. On the other hand, as noted above, several lines of evidence suggest that the lithosphere in oceanic transforms is weaker than the surrounding lithosphere. If this view is correct, then the oceanic lithosphere in active transforms must increase in strength after passing the ridge-transform intersection. Nearly half the earthquakes occurred in lithosphere between 3 and 10 m.y. old; the failure to detect the signature of weak fracture zones requires that strength recovery occur within a few million years. This result is in agreement with the inference of Wessel and Haxby [1990], from their study of geoid and bathymetric profiles over large-offset fracture zones, that full welding occurs 2–4 m.y. after passage of the material of the fracture zone outside of the active transform.

The mechanism through which a transform fault zone experiences a (hypothetical) reduction in strength is highly speculative, and the process by which strength could be recovered is even more obscure. Many workers have suspected that the mechanical behavior of oceanic transforms is influenced by such hydrothermal alteration products as serpentine. Dengo and Logan [1981] report evidence that the lizardite polymorph of serpentine, one of the more likely to occur in an oceanic environment [e.g., Coleman, 1971; Bonatti and Hamlyn, 1981], has a reduced frictional strength as compared with rocks that obey Byerlee's law. The key to strength recovery of the fault zone material could lie in the response of a serpentinized fault zone to the reheating experienced as it passes the ridge-transform intersection. Both the degree of reheating and its consequences could be quite variable, depending on spreading rate, transform length, and the particular characteristics of the adjacent ridge segment.

Several other mechanisms besides reheating may influence the evolution of the strength of a fracture zone. The

cracks and faults which permit extensive circulation of water in the active transform region may, over time, become filled with hydrothermal deposits or sediments. Pore pressure changes are likely to result, particularly in association with fault-zone reheating. Rapid magmatic underplating of the fracture zone near the ridge-transform intersection could also contribute to an increase in effective strength.

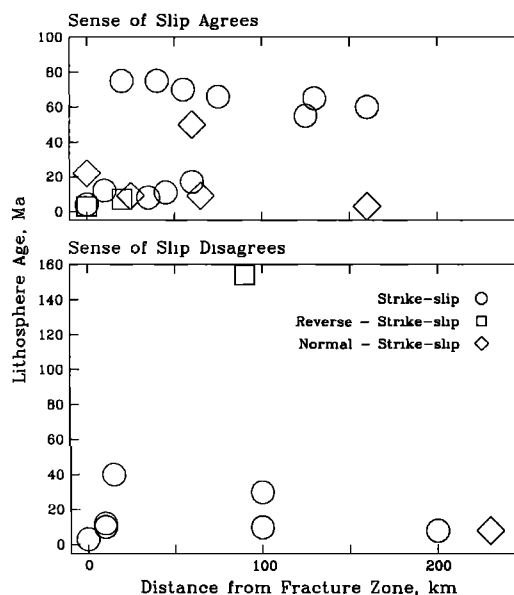
Localized Stresses on Oceanic Fracture Zones

The lithospheric blocks bounding a fracture zone have different cooling rates, creating a potential for stress accumulation at the fracture zone [DeLong *et al.*, 1977]. Both dip-slip and strike-slip components of faulting are expected if the resulting stresses are relieved by faulting. Intraplate earthquakes with locations and focal mechanisms consistent with this hypothesis have been reported by Anderson *et al.* [1974], Forsyth [1975], and Engeln *et al.* [1986].

In the case of dip-slip motion the younger lithosphere should subside relative to the older side. If lithospheric cooling produces a significant component of extension parallel to the ridge [Sandwell, 1986], earthquakes driven by differential subsidence should have normal-faulting mechanisms with fault planes dipping toward the younger side. This hypothesis cannot be tested directly for earthquakes with pure normal-faulting mechanisms because we do not know which nodal plane corresponds to the fault plane. Several lines of evidence suggest, however, that differential subsidence at fracture zones is not a significant cause of intraplate seismicity. A reasonable, but still uncertain choice of the fault plane can be made for the six earthquakes with mixed normal and strike-slip mechanisms having only one nodal plane close to the strike of the fracture zone. With this nodal plane chosen as the fault plane the earthquakes are evenly divided between those dipping toward the younger and older sides of the fracture zone. Normal-faulting earthquakes display very weak evidence, at best, of a preferred orientation with nodal planes subparallel to the fracture zone at short distances from the fracture zone (Figure 3). Also, they are less likely than those with reverse-faulting mechanisms to be clustered near fracture zones (Figures 2 and 3).

DeLong *et al.* [1977] also noted the possibility that differential horizontal thermal contraction at fracture zones could be relieved by strike-slip faulting. The sense of slip in such earthquakes would be the same as the offset of isochrons on the fracture zone. This prediction is based on the assumption that the lithosphere on either side of the fracture zone is effectively pinned far from the ridge, and the contraction of each band of lithosphere is compensated by the production of new lithosphere at the ridge axis. For each of the 30 strike-slip earthquakes with a nodal plane within 20° of the strike of the nearest fracture zone, the sense of slip on the presumed fault plane is compared with the offset of isochrons. These data are presented in Figure 7, with each earthquake plotted according to its distance from the fracture zone and the age of the lithosphere at the epicenter. The sense of slip and isochron offset agree in 20 cases (67%); the percentage is slightly higher (76%) for 17 earthquakes within 50 km of the fracture zone. Some of these events occurred where the lithosphere bounding the fracture zone is as much as 75 m.y. old, however, where differential cooling should be a negligible source of stress.

A large fraction (70%) of the earthquakes with strike-slip



rates were predicted to drop abruptly to approximately 10^{-2} mm/yr and decline slowly with increasing age (e.g., to 2×10^{-3} mm/yr at 50 m.y. in their example).

The effect of differential horizontal contraction was described only qualitatively by DeLong *et al.* [1977]. We make a simple estimate of the magnitude of the strain rate characteristic of this deformation, for comparison with the rate of differential subsidence. The rate of cooling at 1-km increments in depth from the seafloor to the depth of the 1350°C isotherm is calculated from the plate model of Parsons and Sclater [1977]. From these values the average cooling rate for lithospheric columns at 1-m.y. age increments between ages of 1 and 99 m.y. is calculated. Average cooling rates range from 250° to 2°C/m.y. over this age range. These cooling rates are converted to horizontal strain rates with a coefficient of linear thermal expansion of 10^{-5}C^{-1} , a value typical of mantle materials. A half-spreading rate of 10 mm/yr is assumed in order to provide a length scale: a band of lithosphere spanning 1 m.y. in age is 10 km wide. Differential contraction rates at various points along a fracture zone are found by differencing the contraction rates, integrated from the lithosphere on either side out to very old lithosphere. For convenience we integrate the contraction to an age of 100 m.y. for both strips.

For a transform offset of 25 m.y., differential contraction rates range from 10^{-1} mm/yr at 1 m.y. past the ridge-transform intersection to 10^{-2} mm/yr at 50 m.y. We conclude from this highly simplified model that the unrestrained rate of differential horizontal contraction may be as much as an order of magnitude greater than the rate of differential subsidence along oceanic fracture zones. This could account for the relative prominence in our data set of seismicity which could be associated with differential horizontal contraction at fracture zones compared with events indicative of differential subsidence.

CONCLUSIONS

The role of fracture zones in controlling the locus and nature of intraplate strain is investigated using a suite of 77 earthquakes chosen to be representative of the style of faulting at distinct sites of oceanic intraplate seismicity. The focal mechanisms of these events are compared with the trends of well-mapped fracture zones in the epicentral region.

Earthquakes with dip-slip mechanisms display a weak tendency to occur near fracture zones. The mechanisms of reverse-faulting events have no preferred orientation with respect to fracture zones; there is only weak evidence that the nodal planes of normal-faulting earthquakes tend to be aligned parallel to the fracture zone. One nodal plane of earthquakes with strike-slip mechanisms tends to be aligned with nearby fracture zones, but we cannot be sure that the nodal plane in closest alignment with the fracture zone is always the true fault plane. Strike-slip events are not clustered near fracture zones. Among strike-slip earthquakes, the sense of slip in about three fourths of the cases is consistent with the release of horizontal shear stresses arising from differential cooling and contraction of the lithosphere bounding the fracture zone.

The orientations of horizontal stress axes have no preferred orientation with respect to nearby fracture zones. Some degree of alignment would be expected if fracture

zones were substantially weaker than the surrounding lithosphere. Also, we see little evidence for a ridge-perpendicular component of compressional stress contributed by ridge topography or a ridge-parallel component of extensional stress due to thermal contraction. Lateral variations in hydrothermal cooling and differential stress relaxation through both brittle and ductile mechanisms probably introduce horizontal variations in the stress field which are large enough to mask the contribution of these ridge geometry-related stresses in our admittedly small data set. While a larger data set might reveal a contribution from these large-scale effects, our results suggest that they rarely dominate the stress field at any particular site.

Several instances in which some aspect of oceanic intraplate seismicity seems to be correlated with fracture zones suggest that fracture zones may indeed play some role in localizing or controlling the style of deformation. We largely discount these results, however, because they do not consistently point to any of the widely held hypotheses concerning the state of stress and internal deformation of oceanic lithosphere. It may be that these hypotheses are simply wrong and that our results reflect an unrecognized mode of deformation in oceanic lithosphere, but marginally significant, mutually inconsistent results are to be expected from the application of simple statistical measures to small sets of data which are known to be susceptible to bias. In our view the few positive correlations in this study are no stronger than should be expected from such "noisy" processes.

These results support the view that the strength of the lithosphere in most oceanic fracture zones is comparable to that of the surrounding oceanic lithosphere. If the lithosphere in the active transform is substantially weaker than undisturbed lithosphere, strength recovery occurs within a few million years after passage from the active transform to the inactive fracture zone domain. Any remaining strength deficit in fracture zones is too small, in comparison with variations in the strength and level of stress in oceanic lithosphere arising from other causes, to have an observable influence on oceanic intraplate seismicity. Thus the available data suggest that the nontransform limbs of fracture zones have at most a minor influence on the large-scale mechanical properties of the oceanic lithosphere and the intraplate stress field in oceanic regions.

Acknowledgments. We thank Jeff Karson and Marc Parmentier for helpful discussions and Cecily Wolfe for assistance with Figure 1. The paper benefited from thoughtful reviews by Daniel Walker, Bill Spence, Steve Mueller, and an anonymous reviewer. This research was supported by the National Science Foundation under grants EAR-8817173 and EAR-9004750 and by the National Aeronautics and Space Administration under grants NAG 5-814 and NAG 5-1921.

REFERENCES

- Abbott, D., A statistical correlation between ridge crest offsets and spreading rate, *Geophys. Res. Lett.*, *13*, 157-160, 1986.
- Aki, K., and P. G. Richards, *Quantitative Seismology: Theory and Methods*, vol. 1, p. 114, W. H. Freeman, New York, 1980.
- Anderson, R. N., D. W. Forsyth, P. Molnar, and J. Mammerrickx, Fault plane solutions of earthquakes on the Nazca plate boundaries and the Easter plate, *Earth Planet. Sci. Lett.*, *24*, 188-202, 1974.
- Artyushkov, E. V., Stresses in the lithosphere caused by crustal thickness inhomogeneities, *J. Geophys. Res.*, *78*, 7675-7708, 1973.

- Atwater, T., and J. Severinghaus, Tectonic map of the northeast Pacific Ocean, *Geol. Soc. Am.*, Boulder, Colo., 1988a.
- Atwater, T., and J. Severinghaus, Tectonic map of the east central Pacific Ocean, *Geol. Soc. Amer.*, Boulder, Colo., 1988b.
- Atwater, T., and J. Severinghaus, Tectonic map of the north central Pacific Ocean, *Geol. Soc. Amer.*, Boulder, Colo., 1988c.
- Bergman, E. A., Intraplate earthquakes and the state of stress in oceanic lithosphere, *Tectonophysics*, 132, 1–35, 1986.
- Bergman, E. A., and S. C. Solomon, Oceanic intraplate earthquakes: Implications for local and regional intraplate stress, *J. Geophys. Res.*, 85, 5389–5410, 1980.
- Bergman, E. A., and S. C. Solomon, Source mechanisms of earthquakes near mid-ocean ridges from body waveform inversion: Implications for the early evolution of oceanic lithosphere, *J. Geophys. Res.*, 89, 11,415–11,441, 1984.
- Bergman, E. A., and S. C. Solomon, Earthquake source mechanisms from body-waveform inversion and intraplate tectonics in the northern Indian ocean, *Phys. Earth Planet. Inter.*, 40, 1–23, 1985.
- Bergman, E. A., J. L. Nabelek, and S. C. Solomon, An extensive region of off-ridge normal-faulting earthquakes in the southern Indian Ocean, *J. Geophys. Res.*, 89, 2425–2443, 1984.
- Bergman, E. A., S. C. Solomon, W. S. D. Wilcock, and G. M. Purdy, On the seismic width of the transform fault zone of the Kane Fracture Zone (abstract), *Eos Trans. AGU*, 69, 476, 1988.
- Bonatti, E., and P. R. Hamlyn, Oceanic ultramafic rocks, in *The Sea*, vol. 7, *The Oceanic Lithosphere*, edited by C. Emiliani, pp. 241–283, John Wiley, New York, 1981.
- Bratt, S. R., E. A. Bergman, and S. C. Solomon, Thermoelastic stress: How important as a cause of earthquakes in young oceanic lithosphere?, *J. Geophys. Res.*, 90, 10,249–10,260, 1985.
- Brune, J. N., T. L. Henyey, and R. F. Roy, Heat flow, stress, and rate of slip along the San Andreas fault, California, *J. Geophys. Res.*, 74, 3821–3827, 1969.
- Bulmer, M. G., *Principles of Statistics*, 252 pp., Dover, Mineola, New York, 1979.
- Cande, S. C., J. L. LaBrecque, R. L. Larson, W. C. Pittman, III, X. Golovchenko, and W. F. Haxby, Magnetic lineations of the world's ocean basins (map), *Am. Assoc. Pet. Geol.*, Tulsa, Okla., 1989.
- Coleman, R. G., Petrologic and geophysical nature of serpentinites, *Geol. Soc. Am. Bull.*, 82, 897–918, 1971.
- Collette, B. J., Thermal contraction joints in spreading seafloor as origin of fracture zones, *Nature*, 251, 299–300, 1974.
- Dahlen, F. A., Isostasy and the ambient state of stress in the oceanic lithosphere, *J. Geophys. Res.*, 86, 7801–7807, 1981.
- DeLong, S. E., J. F. Dewey, and P. J. Fox, Displacement history of oceanic fracture zones, *Geology*, 5, 199–202, 1977.
- Dengo, C. A., and J. M. Logan, Implications of the mechanical and frictional behavior of serpentinite to seismogenic faulting, *J. Geophys. Res.*, 86, 10,771–10,782, 1981.
- Denlinger, R. P., A model for large-scale plastic yield of the Gorda deformation zone, *J. Geophys. Res.*, in press, 1992.
- Dziewonski, A. M., T.-A. Chou, and J. H. Woodhouse, Determination of earthquake source parameters from waveform data for studies of global and regional seismicity, *J. Geophys. Res.*, 86, 2825–2852, 1981.
- Dziewonski, A. M., G. Ekström, J. E. Franzen, and J. H. Woodhouse, Global seismicity of 1977: Centroid-moment tensor solutions for 471 earthquakes, *Phys. Earth Planet. Inter.*, 45, 11–36, 1987.
- Engeln, J. F., D. A. Wiens, and S. Stein, Mechanisms and depths of Atlantic transform earthquakes, *J. Geophys. Res.*, 91, 548–577, 1986.
- Forsyth, D. W., Fault plane solutions and tectonics of the south Atlantic and Scotia Sea, *J. Geophys. Res.*, 80, 1429–1443, 1975.
- Fredrich, J., R. McCaffrey, and D. Denham, Source parameters of seven large Australian earthquakes determined by body waveform inversion, *Geophys. J.*, 95, 1–13, 1988.
- Froidevaux, C., Energy dissipation and geometric structure at spreading plate boundaries, *Earth Planet. Sci. Lett.*, 20, 419–424, 1973.
- Hanks, T. C., and C. B. Raleigh, The conference on magnitude of deviatoric stresses in the Earth's crust and uppermost mantle, *J. Geophys. Res.*, 85, 6083–6085, 1980.
- Haxby, W. F., and E. M. Parmentier, Thermal contraction and the state of stress in oceanic lithosphere, *J. Geophys. Res.*, 93, 6419–6429, 1988.
- Hickman, S. H., Stress in the lithosphere and the strength of active faults, *Rev. Geophys.*, *Suppl.*, 29, part 2, 759–775, 1991.
- Lachenbruch, A. H., and J. H. Sass, Heat flow and energetics of the San Andreas fault zone, *J. Geophys. Res.*, 85, 6185–6222, 1980.
- Lachenbruch, A. H., and G. A. Thompson, Oceanic ridges and transform faults: Their intersection angles and resistance to plate motion, *Earth Planet. Sci. Lett.*, 15, 116–122, 1972.
- Lay, T., and E. A. Okal, The Gilbert Islands (Republic of Kiribati) earthquake swarm of 1981–83, *Phys. Earth Planet. Inter.*, 33, 284–303, 1983.
- Lowrie, A., C. Smoot, and R. Batiza, Are oceanic fracture zones locked and strong or weak?: New evidence for volcanic activity and weakness, *Geology*, 14, 242–245, 1986.
- McKenzie, D. P., The relation between fault plane solutions for earthquakes and the directions of the principal stresses, *Bull. Seismol. Soc. Am.*, 59, 591–601, 1969.
- McNutt, M. K., K. Fisher, S. Kruse, and J. Natland, The origin of the Marquesas Fracture Zone and its implications for the nature of hotspots, *Earth Planet. Sci. Lett.*, 91, 381–393, 1989.
- Mount, V. S., and J. Suppe, State of stress near the San Andreas fault: Implications for wrench tectonics, *Geology*, 5, 1143–1146, 1987.
- Oldenburg, D. W., and J. N. Brune, An explanation for the orthogonality of ocean ridges and transform faults, *J. Geophys. Res.*, 80, 2575–2585, 1975.
- Parmentier, E. M., and W. F. Haxby, Thermal stresses in the oceanic lithosphere: Evidence from geoid anomalies at fracture zones, *J. Geophys. Res.*, 91, 7193–7204, 1986.
- Parsons, B., and J. G. Sclater, An analysis of the variation of ocean floor bathymetry and heat flow with age, *J. Geophys. Res.*, 82, 803–827, 1977.
- Richardson, R. M., S. C. Solomon, and N. H. Sleep, Intraplate stress as an indicator of plate tectonic driving forces, *J. Geophys. Res.*, 81, 1847–1856, 1976.
- Richardson, R. M., S. C. Solomon, and N. H. Sleep, Tectonic stress in the plates, *Rev. Geophys.*, 17, 981–1019, 1979.
- Sandwell, D. T., Thermal stress and the spacings of transform faults, *J. Geophys. Res.*, 91, 6405–6417, 1986.
- Sandwell, D. T., and G. Schubert, Lithospheric flexure at fracture zones, *J. Geophys. Res.*, 87, 4657–4667, 1982.
- Scholz, C. H., Mechanics of faulting, *Ann. Rev. Earth Planet. Sci.*, 17, 309–334, 1989.
- Sclater, J. G., C. Jaupart, and D. Galson, The heat flow through oceanic and continental crust and the heat loss of the Earth, *Rev. Geophys.*, 18, 269–311, 1980.
- Severinghaus, J. P., and K. C. Macdonald, High inside corners at ridge-transform intersections, *Mar. Geophys. Res.*, 9, 353–367, 1988.
- Sykes, L. R., Intraplate seismicity, reactivation of preexisting zones of weakness, alkaline magmatism, and other tectonism postdating continental fragmentation, *Rev. Geophys.*, 16, 621–688, 1978.
- Sykes, L. R., and M. L. Sbar, Intraplate earthquakes, lithospheric stresses and the driving mechanism of plate tectonics, *Nature*, 245, 298–302, 1973.
- Turcotte, D. L., Are transform faults thermal contraction cracks?, *J. Geophys. Res.*, 79, 2573–2577, 1974.
- Wessel, P., and W. F. Haxby, Thermal stresses, differential subsidence, and flexure at oceanic fracture zones, *J. Geophys. Res.*, 95, 375–391, 1990.
- Wiens, D. A., and D. E. Petroy, Historical seismicity and implications for diffuse plate convergence in the northeast Indian Ocean, *J. Geophys. Res.*, 94, 12,301–12,320, 1989.
- Wiens, D. A., and D. E. Petroy, The largest recorded earthquake swarm: Intraplate faulting near the Southwest Indian Ridge, *J. Geophys. Res.*, 95, 4735–4750, 1990.
- Wiens, D. A., and S. Stein, Age dependence of oceanic intraplate seismicity and implications for lithospheric evolution, *J. Geophys. Res.*, 88, 6455–6468, 1983.
- Wiens, D. A., and S. Stein, Intraplate seismicity and stresses in young oceanic lithosphere, *J. Geophys. Res.*, 89, 11,442–11,464, 1984.
- Wilcock, W. S. D., G. M. Purdy, and S. C. Solomon, Microearthquake evidence for extension across the Kane transform fault, *J. Geophys. Res.*, 95, 15,439–15,462, 1990.

- Zoback, M. D., et al., New evidence on the state of stress of the San Andreas fault system, *Science*, 238, 1105-1111, 1987.
- Zoback, M. L., et al., Global patterns of tectonic stress, *Nature*, 341, 291-298, 1989.
- Institution of Washington, 5241 Broad Branch Road, Washington, D. C. 20015-1305.

E. A. Bergman, U.S. Geological Survey, P.O. Box 25046, Mail Stop 967, Denver Federal Center, Denver, CO 80225.
S. C. Solomon, Department of Terrestrial Magnetism, Carnegie

(Received October 28, 1991;
revised May 4, 1992;
accepted May 6, 1992.)